processes

MDPI

Article

Evaluation of the Adsorption Efficiency on the Removal of Lead(II) Ions from Aqueous Solutions Using *Azadirachta indica* Leaves as an Adsorbent

Abubakr Elkhaleefa [1,2], Ismat H. Ali [3,*], Eid I. Brima [3,4], Ihab Shigidi [1], Ahmed. B. Elhag [5,6] and Babiker Karama [7]

1 Department of Chemical Engineering, College of Engineering, King Khalid University, Abha 61413, Saudi Arabia; amelkhalee@kku.edu.sa (A.E.); etaha@kku.edu.sa (I.S.)
2 Department of Chemical Engineering and Chemical Technology, University of Gezira, Wadmedani 21113, Sudan
3 Department of Chemistry, College of Science, King Khalid University, Abha 61413, Saudi Arabia; ebrima@kku.edu.sa
4 School of Allied Health Science, De Montfort University, The Gateway, Leicester LE1 9BH, UK
5 Department of Civil Engineering, College of Engineering, King Khalid University, Abha 61413, Saudi Arabia; abalhaj@kku.edu.sa
6 Department of Geology, Faculty of Science, Kordofan University, Elobied 51111, Sudan
7 Department of Chemical Engineering, Karary University, Khartoum 14411, Sudan; babikerka@hotmail.com
* Correspondence: ismathassanali@gmail.com

Citation: Elkhaleefa, A.; Ali, I.H.; Brima, E.I.; Shigidi, I.; Elhag, A..B.; Karama, B. Evaluation of the Adsorption Efficiency on the Removal of Lead(II) Ions from Aqueous Solutions Using *Azadirachta indica* Leaves as an Adsorbent. *Processes* **2021**, *9*, 559. https://doi.org/10.3390/pr9030559

Academic Editors: Monika Wawrzkiewicz and Anna Wołowicz

Received: 2 February 2021
Accepted: 24 February 2021
Published: 23 March 2021

Abstract: The efficiency of *Azadirachta indica* (neem leaves) on the removal of Pb(II) ions by adsorption from aqueous solution was investigated in this study. The efficiency of these leaves (without chemical or thermal treatment) for the adsorption of Pb(II) ions has not previously been reported. Batch experiments were performed to study the effect of the particle size, pH, adsorbent dose, contact time, initial Pb(II) ion concentration, and temperature. The maximum removal of 93.5% was achieved from an original Pb(II) ion solution concentration of 50 mg/L after 40 min, at pH 7, with 0.60 g of an adsorbent dose. The maximum adsorption capacity recorded was 39.7 mg/g. The adsorption process was also studied by examining Langmuir, Freundlich, Temkin isotherm, and Dubinin–Radushkevich (D-R) isotherm models. The results revealed that the adsorption system follows the pseudo-second-order model and fitted the Freundlich model. Several thermodynamic factors, namely, the standard free energy (ΔG°), enthalpy (ΔH°), and entropy (ΔS°) changes, were also calculated. The results demonstrated that the adsorption is a spontaneous, physical, and exothermic process. The surface area, pore size, and volume of adsorbent particles were measured and presented using a surface area analyzer (BET); the morphology was scanned and presented with the scanning electron microscope technique (SEM); and the functional groups were investigated using μ-FTIR.

Keywords: biosorption; isotherms; lead (II); *Azadirachta indica* leaves

1. Introduction

Industrial activities have significantly contributed to environmental pollution. Toxic metals are one of the major pollutants causing serious damage to the environment, in addition to being a documented source of many diseases [1]. The heavy metal pollutants in wastewater are highly toxic, hazardous to plants and animals, and result in a shortage of clean water [2,3]. Lead is among these toxic elements, and has acute and chronic health effects on humans [4]. Lead pollution affected nearly 18–22 million people in 2010, motivating an investigation of water purification processes [5].

With respect to metal removal, wastewater purification includes various methods, such as biosorption, adsorption, electrochemical treatments, and oxidation [6,7]. Heavy metal biosorption is one of the favorable fields of remedy due to the low cost and easy

accessibility of raw materials, as well as their eco-friendly nature [8]. Other benefits of biosorption are the selectivity for particular metals; low operational time; and most importantly, the absence of chemical waste generation [9]. Different types of cheap plant materials have been investigated as prospective biosorbents for heavy metals [10].

Biosorption is known to be more effective in removing lead metal contaminants from aqueous solutions, where the efficiency rate in batch adsorption tests is higher than 90% [11]. However, the success of biosorption in the removal of lead metal from wastewater depends on several experimental parameters, such as the temperature, pH, and original solution metal concentration [12,13]. The biosorption removal of Pb(II) ions using natural biosorbent from cactus cladodes revealed that the particle size, mass of biosorbent, and contact time are additional factors influencing the operation success [14]. The optimum biosorption of Pb(II) ions increases with an increase in the biosorbent particle size and dosage [14,15]. Various natural materials have been used for lead removal. These include pumpkin seeds, bamboo, cocoa shells, coconut shell, calotropis roots, peanut shells, Moringa bark, orange bark, cashew nut shells, and activated carbon (maize tassel, periwinkle shells, oil palm, and rice husk) [16,17]. Other natural materials have been reported to be efficient sorbents for various pollutants. *Platanus orientalis* leaf powder was used as an efficient sorbent for Cu(II) ion removal from aqueous solutions. The maximum adsorption capacity for this material was determined to be 49.94 mg/g [18]. *Urtica* has been reported as an effective sorbent for the removal of Methylene Blue dye from aqueous solutions, with a maximum adsorption capacity of 101.01 mg/g [19].

The chemical screening of neem leaves showed positive results for steroids, saponins, flavonoids, alkaloids, tannins, and amino acid [20]. Most of these constituents possess electron withdrawing groups which may enhance the adsorption capacity of the neem leaves.

This study aims to evaluate *Azadirachta indica* leaves' powder (AILP) as an eco-friendly, efficient, and cheap biosorbent for Pb(II) ion removal.

2. Materials and Methods

2.1. Preparation and Adsorption Processes

Azadirachta indica (neem leaves) samples were collected from Jizan city, south of Saudi Arabia, and washed with deionized and distilled water. Then samples were dried at room temperature. The leaves were ground by a grinder into powder form, before being sieved. A stock solution of 50 mg/L was prepared using $Pb(NO_3)_2$ (Sigma-Aldrich, Saint Louis, MissourI, USA, ACS reagent $\geq$ 99%.)

2.2. Batch Adsorption Experiment

Batch experiments were performed using 250 mL stoppered bottles containing the desired mass at a pH of 5.5 with 50 mL of Pb(II) solution (50 mg/L). The mixture was shaken at 298 K (except when examining the temperature effect) by a temperature-controlled water bath shaker. At the end of the shaking time, the solid adsorbent was isolated from the solution by filtration, and the remaining concentration of Pb(II) ions was then determined using an atomic absorption spectrometer (AAS) (SpectrAA 220, Varian, UK). Parameters influencing the sorption efficiency were investigated by changing one factor and keeping the others constant. The adsorption extent was determined using Equation (1):

$$q_e = \frac{C_o - C_e}{M} \times V, \quad (1)$$

where V is the volume of the Pb(II) solution in the bottle, q_e is the metal uptake capacity (mg/g), M is the mass of AILP (g), C_o is the initial Pb(II) concentration, and C_e is the Pb(II) concentration at equilibrium. The total removal efficiency (R%) was calculated using Equation (2).

$$R\% = \frac{C_o - C_e}{C_o} \times 100 \quad (2)$$

The investigated parameters, including the particle size, shaking time, mass of adsorbent, temperature, and solution concentration, were investigated.

2.3. Characterization of AILP

The surface area, pore-volume, and pore size were investigated using a Quanta Chrome NOVA 4200E Surface Area Analyzer. The morphology of the powder was examined using a Jeol 6360 (Japan) scanning electron microscope at an accelerating voltage of 20 kV. The functional groups of the powder before and after adsorption were investigated by μ-FT-IR (Cary 630 FTIR from Agilent, Santa Clara, USA) in the range of 400–4000 cm^{-1} at a spectral resolution of 8 cm^{-1}.

2.4. Reusability of AILP

AILP was reactivated by vigorous shaking in an excess quantity of de-ionized water for 12 hrs. AILP was separated by filtration and then dried by heating it overnight at 105 °C. The optimal conditions were maintained throughout all reusability experiments.

3. Results

3.1. Characterization of AILP

3.1.1. Surface Area of AILP

The AILP sample exhibited a high surface area of 183 m^2/g, enhancing its adsorption capabilities. The results revealed that the average pore diameter is 10.3 nm and the total pore volume is 0.355 cm^3/g. Comparative data are given in Table 1. These data demonstrate that the AILP surface area is larger than that of the reported sorbents, indicting a high adsorption capacity.

Table 1. The surface area, total pore volume, and average pore diameter for various adsorbents.

Adsorbent	Surface Area (m^2/g)	Total Pore Volume (cm^3/g)	Average Pore Diameter (nm)	Reference
AILP	183	0.335	10.3	This study
Date seeds	124	0.469	9.8	[21]
P(AN-AA)/AMP composite	39	0.35	34.4	[22]
Red clay	35	0.57	6.5	[23]
Modified sugarcane	7	0.15	Not reported	[24]

3.1.2. IR Spectrum

The μ-FT-IR spectrum is used to estimate the contribution of functional groups on the adsorbent surface in the adsorption process. The FT-IR analysis was performed before and after the adsorption process (Figure 1). The results revealed distinguished bands of Pb-O stretching vibrations that appeared at 462 cm^{-1} and OH stretching of the hydroxide groups. These bands may confirm the adsorption of Pb(II) ions on the adsorbent surface. Other bands appeared at 1298, 1350, and 1723 cm^{-1}, and these bands are probably related to the stretching of -C-N-, -C=N-, and -C=C-, respectively, in polyheterocycles. However, the FT-IR spectra of the adsorbent before and after adsorption were very similar due to the physisorption process.

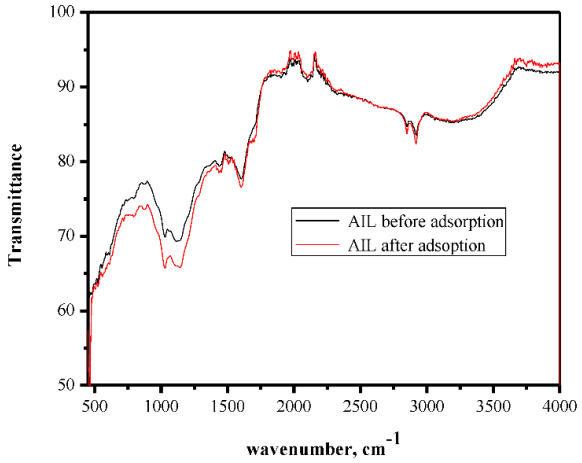

Figure 1. FT-IR spectrum of *Azadirachta indica* leaves' powder (AILP) before and after adsorption.

3.1.3. Scanning Electron Microscope (SEM)

The SEM images of AILP before and after adsorption are presented in Figure 2. The SEM images illustrate differences in the surface morphologies of the AILP surfaces before and after adsorption. The surface of the AILP before adsorption showed micro flakes with an approximate size of 0.5 µm (Figure 2a). Additionally, the analysis of the AILP surface after adsorption revealed differences in the surface structure and the adsorption process led to the formation of many floccules and spots due to the adsorption of Pb(II) ions on the AILP surface, leading to a rough appearance.

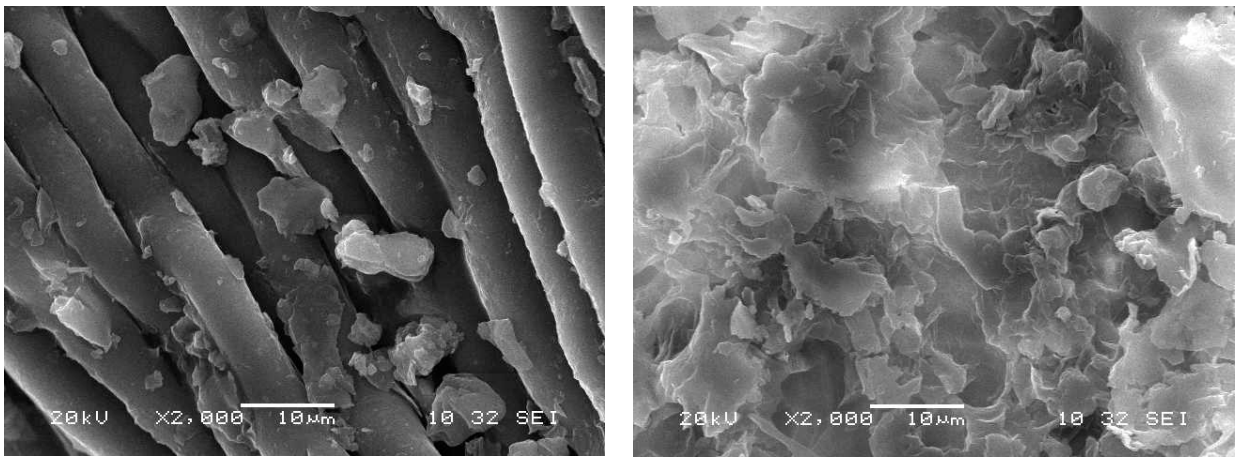

(**a**) (**b**)

Figure 2. Scanning Electron Microscope (SEM) images of the AILP surface (**a**) before and (**b**) after adsorption.

3.2. Effect of the Adsorbent Particle Size

The removal efficiency of Pb(II) ions from aqueous solutions by the AILP increased from 82.9% to 99.1% as the AILP size decreased from 800 to 100 µm, at 298 K, for a 50 mg/L initial Pb(II) ions concentration (Figure 3). With a decrease in AILP particle sizes, the surface area of the AILP increased, so the number of active sites accessible on the AILP surface had a better exposure to the adsorbate. Similar findings have also been reported by other researchers [12].

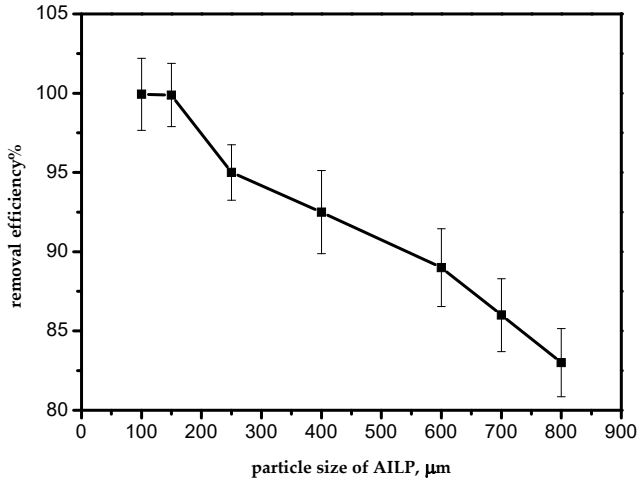

Figure 3. Effect of the adsorbent particle size.

3.3. Effect of the pH

The maximum adsorption was achieved at pH 5.0 (Figure 4). It is presidentially noted that with a pH higher than 5.0, the adsorption activity decreased sharply. However, at pH values lower than 5.0, the adsorption process could be hindered by the existence of a high concentration of positive hydrogen ions, and the adsorption sites became positively charged, exerting a repelling effect on the Pb(II) cations. With an increase in the pH, the negative charge density on AILP increased as a result of deprotonation of the metal-binding sites, hence increasing the metal uptake; such findings are in agreement with previous studies. It is well-known that lead ions start to precipitate above pH 5.0–6.0 in the form of $Pb(OH)_2$, suppressing the adsorption of lead ions [1].

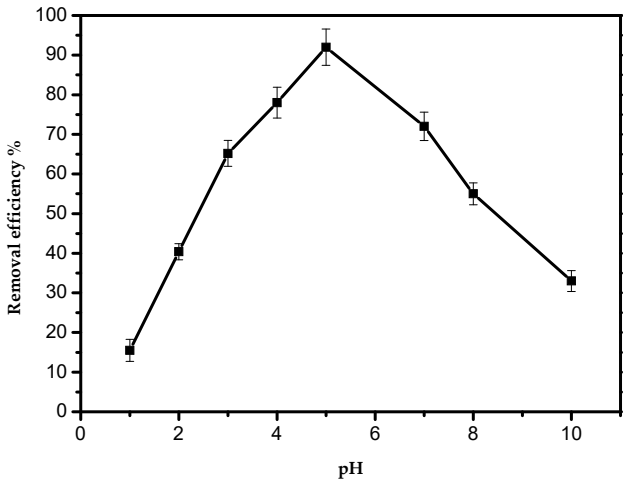

Figure 4. Effect of the pH on the removal efficiency of Pb(II) ions by AILP.

3.4. Effect of the Adsorbent Dosage

To investigate the effect of the sorbent mass on the efficiency of the adsorption process, a series of batch experiments were conducted with various sorbent masses of 0.05, 0.10, 0.20, 0.30, 0.40, 0.60, 0.80, and 1.0 g per 50 mL of aqueous solution of Pb(II) ions. The effect is presented in Figure 5. As the mass of the sorbent increased, the adsorption efficiency also increased. This can be attributed to an increase in the AILP surface area with its mass. The maximum adsorption efficiency for Pb(II) ions was achieved at 0.60 g/50 mL. From the results, it is clear that an increase in the adsorbent mass above 0.6 g had no effect on the adsorption efficiency of Pb(II) ions from the aqueous solution.

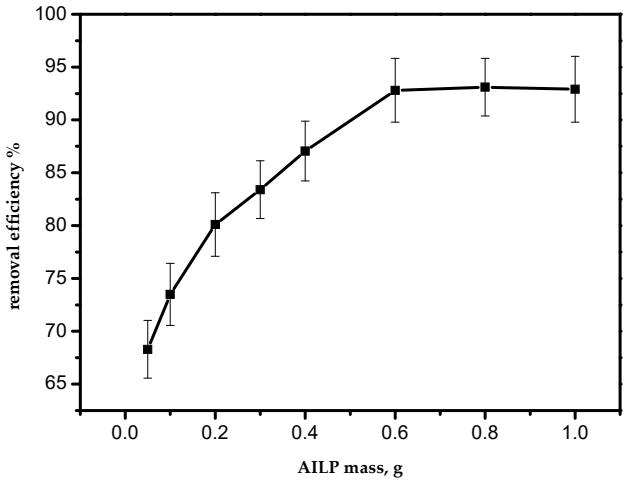

Figure 5. Effect of the adsorbent mass on the removal efficiency of Pb(II) ions by AILP.

3.5. Effect of the Agitation Time

The effect of the agitation time on the adsorption of Pb(II) ions using the AILP is presented in Figure 6. The results showed that the time of 40 min was sufficient for achieving the optimum adsorption, without any influence from increasing the contact time. As demonstrated in Figure 6, the adsorption process could be divided into three phases. The first phase was significantly fast, representing about 88% removal within 30 min. The second phase showed slower adsorption. The first stage was caused by the large surface area of the AILP. With the progressive occupation of these sites, the process became slower in the second stage due to less adsorption sites being available for Pb(II) ions. The third phase was the desorption of Pb(II) ions from the AILP surface. Some of the adsorbed Pb(II) ions might have leached from the AILP into the solution and this is probably a result of the long agitation time.

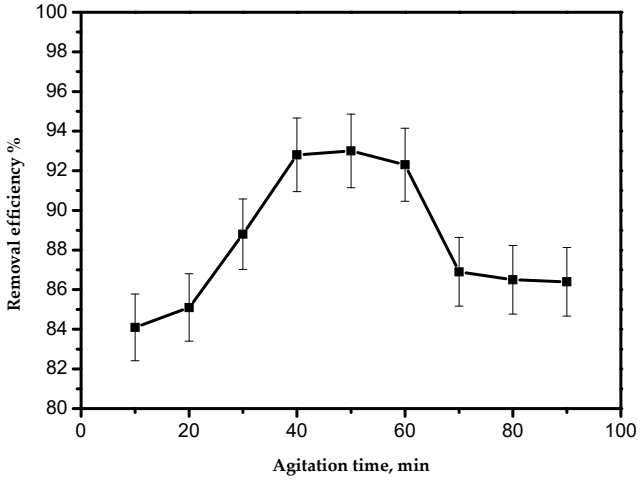

Figure 6. Effect of the agitation time on the removal efficiency of Pb(II) ions by AILP.

3.6. Adsorption Kinetics

The aim of investigating the adsorption kinetics is to explore the mechanism of adsorption and evaluate the efficiency of the adsorbent. The pseudo-first-order, pseudo-second-order, and intra-particle diffusion kinetic models were used to investigate the obtained data on the adsorption of Pb(II) ions on the AILP.

3.6.1. Pseudo-First-Order Kinetic Model

The equation of this model is given by Equation (3):

$$\ln(q_e - q_t) = -kt + \ln q_e, \quad (3)$$

where q_e is the amount of solute (mg/g) removed at equilibrium, q_t is the quantity of solute adsorbed at any time (t), and k is the rate constant. It was found that the data do not fit this model (R^2 = 0.0006).

3.6.2. Pseudo-Second-Order Kinetic Model

The equation of this model is

$$\frac{t}{q_t} = \frac{1}{k_2 q_e^2} + \frac{t}{q_e}. \quad (4)$$

A typical plot of the pseudo-second-order equation is shown in Figure 7. The straight line in the plot proves that the experimental data appropriately obey the pseudo-second-order model. Values of q_e and k_2 were determined from the intercept and slope of Figure 8. These parameters and the correlation coefficient are presented in Table 2. This agrees with previous results and explanations [1,25]. It can be concluded from previous studies that the adsorption kinetics model was governed by the adsorbent nature.

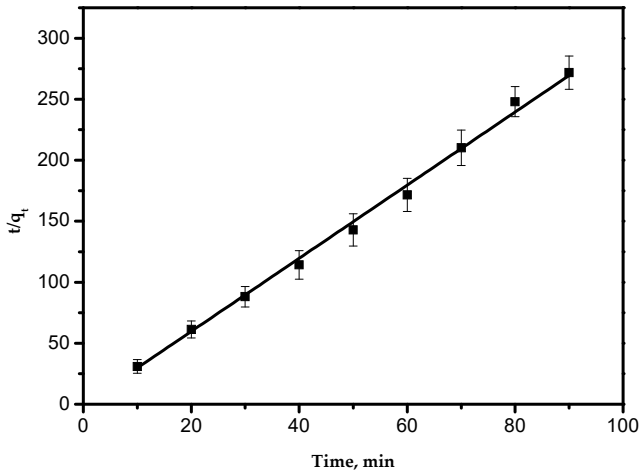

Figure 7. Pseudo-second-order adsorption kinetics.

3.6.3. Intra-Particle Diffusion Kinetic Model

This model is shown by Equation (5):

$$q_t = k_{id}\, t^{1/2} + I, \quad (5)$$

where k_{id} is the intra-particle diffusion rate constant, mg/g/min$^{1/2}$. The value of (k_{id}) was calculated from Equation (5) and is presented in Table 2. The relationship between qt and $t^{1/2}$ was not linear over the entire time range. The first curved part of the plot can be attributed to the boundary layer diffusion effects and it represents intra-particle diffusion controlled by the rate constant k_{id} (Figure 8).

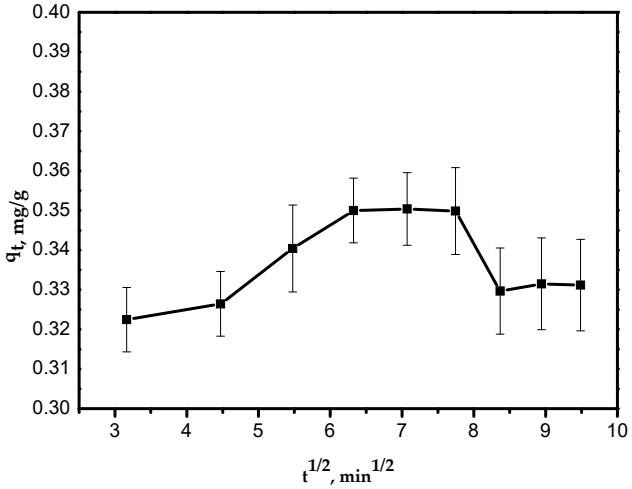

Figure 8. Intra-particle diffusion kinetic model.

Table 2. Kinetic parameters of the removal of Pb(II) ions from aqueous solutions by AILP.

Kinetic Model	Parameters	
Pseudo-second-order model	q_e (mg/g)	3.00
	k_2 (g/mg $min^{(1/2)}$)	0.21
	R^2	0.9976
Intraparticle diffusion model	k_{id} mg/g $min^{(1/2)}$	0.0014
	I	0.328
	R^2	0.07

3.7. Effect of the Initial Pb(II) Concentration

The effect of the initial concentration of Pb(II) ions on the adsorption efficiency is presented in Figure 9, where it is evident that the adsorption efficiency of Pb(II) ions decreased as the initial Pb(II) ion concentration increased. The decrease in adsorption efficiency can be attributed to the deficiency of sufficient adsorption sites for accumulating the large increase of metal ions available in the solution [21].

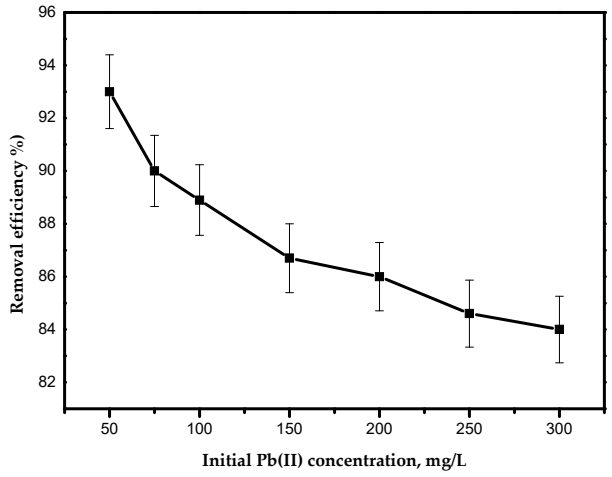

Figure 9. Effect of the initial concentration of Pb(II) ions on the removal efficiency.

3.8. Adsorption Isotherm

The adsorption isotherm models were investigated to explore the interaction mechanism of Pb(II) ions on the adsorbent sites [1,21]. The adsorption isotherm models were

analyzed by specific parameters, whose values express the surface characteristics and affinity of the adsorbent towards heavy metal ion adsorption [21]. Out of numerous isotherm models, four were examined for this study, namely, Freundlich, Langmuir, Temkin, and Dubinin–Radushkevich (D-R) models.

3.8.1. Langmuir Isotherm

Equation (6) presents the Langmuir linear equation:

$$\frac{C_e}{q_e} = \frac{C_e}{q_m} + \frac{1}{bq_m}. \quad (6)$$

The results obtained in this study were fitted to the Langmuir isotherm model to determine the maximum adsorption capacity (q_{max}) of AILP on Pb(II) ions. The linear plot of C_e/q_e vs. C_e (Figure 10a) obtained indicates the applicability of the Langmuir model. Values of b and q_m were calculated graphically from the intercept and slope, respectively, and are presented in Table 3. From the Langmuir isotherm, the adsorption process can be classified as follows: when $R_L = 0$, a favorable process occurs when $0 < R_L < 1$, linear process occurs when $R_L = 1$, and unfavorable process occurs when $R_L > 1$. The R_L values for the initial AILP concentrations were between 0.13 and 0.49, which indicates that the adsorption of Pb(II) ions on AILP is a favorable process.

3.8.2. Freundlich Isotherm

This is an experimental expression used for adsorption on heterogeneous surfaces with the interaction between adsorbed molecules. This model suggests an exponential drop in adsorption energy upon completion of the adsorption centers of the adsorbent. The linear equation of the Freundlich model is shown by Equation (7) [21]:

$$\ln q_e = \ln K_f + \frac{1}{n} \ln C_e, \quad (7)$$

where K_f is the relative adsorption capacity of the adsorbent that is related to the bonding energy and n is the heterogeneity element stating the deviancy from the linearity of adsorption. A plot of ln q_e versus ln C_e was used to confirm the Freundlich adsorption isotherm. Values of K_f and n were calculated from the intercept and slope (Figure 10b) and are tabulated in Table 3. An explanation of n, which controls the relationship between the solution concentration and adsorption, is as follows: If $n < 1$, adsorption is a physical process; if $n = 1$, adsorption is linear; and if $n > 1$, adsorption is a chemical process. The obtained n value was found to be 0.60, indicating physical processes.

3.8.3. Temkin Isotherm

In this model, the heat of adsorption AILP molecules in the layer is supposed to decrease linearly with the coverage of the adsorbent surface because of a reduction in the adsorbate–adsorbent interactions. The model is defined by Equation (8):

$$q_e = B \ln A + B \ln C_e, \quad (8)$$

where $B = (RT)/b_t$, R is the universal gas constant, and T is the temperature in Kelvin. The constant b_t is associated with the heat of adsorption (J/mol). A is the equilibrium binding constant corresponding to the maximum binding energy.

Values of A and B were determined from the slope and intercept of Equation (6) and Figure 10c and are shown in Table 3. The b_t value was 318 J/mol, indicating physical adsorption processes [21].

3.8.4. Dubinin–Radushkevich (D-R) Isotherm

The D-R Isotherm model is commonly used to conclude the mean free energy of the adsorption process [1]. The formula of this model is described by Equation (9):

$$\ln q_e = \ln q_{max} - \beta\varepsilon^2, \quad (9)$$

where ε is defined as

$$\varepsilon = RT \ln\left(\frac{1}{1 + C_e}\right). \quad (10)$$

T denotes the temperature (K), R is the universal gas constant, and q_{max} and β are D-R isotherm constants. β and q_{max} were obtained from the slope and intercept of Equation (9) and Figure 10d and the values are presented in Table 3.

The mean free energy of adsorption process, E_f, is defined as the free energy change when one mole of ions is moved to the solid surface from infinity in solution and was determined from Equation (11).

$$E_f = \frac{1}{\sqrt{2\beta}} \quad (11)$$

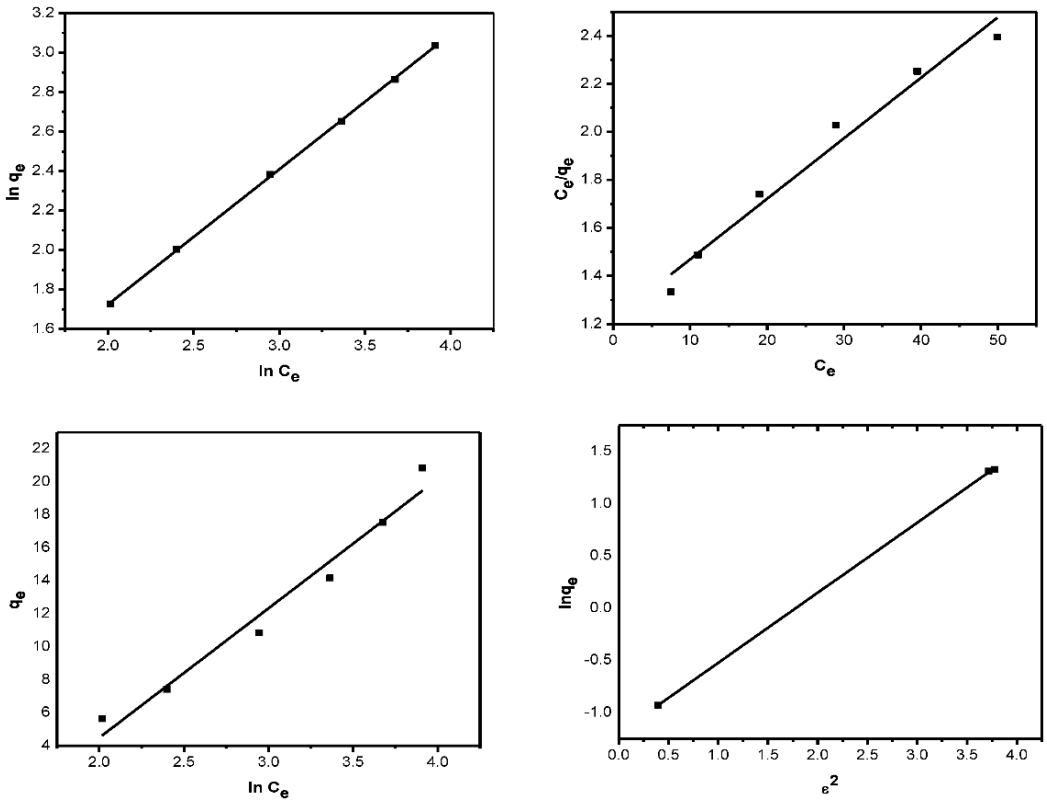

Figure 10. Adsorption isotherm models: (**a**) Langmuir; (**b**) Freundlich; (**c**) Temkin; and (**d**) D-R.

It is well-established that the E_f value is crucial for predicting the adsorption type. For $8 < E_f < 16$ kJ/mol, adsorption is considered a chemisorption process, and, when $E_f < 8$ kJ/mol, adsorption is classified as a physical process. In this study, the lower value of E_f (2.2 KJ/mol) indicates that the adsorption process was of a physical type.

Table 3. Adsorption isotherm constants obtained from the four adsorption isotherm models.

Adsorption Model	Isotherm Constants	Value
Langmuir	q_{max} (mg/g)	39.7
	K_L (L/g)	0.021
	R^2	0.9756
Freundlich	n	0.6
	K_f (mg/g)/(mg/L)	1.0
	R^2	0.9997
Temkin	A (L/g)	1.3
	B	7.8
	R^2	0.9703
D-R	B	1×10^{-7}
	q_{max} (mg/g)	4.05
	R^2	0.9997

3.9. Effect of the Temperature

The temperature effect on the adsorption of Pb(II) ions on AILP was examined at a range from 298 to 318 K and is presented in Figure 11. The results revealed that the adsorption efficiency decreased slightly from 95.9% to 93.4% as the temperature increased from 298 to 318 K. This can be attributed to the possible damage of adsorption sites at elevated temperatures.

3.10. Thermodynamic Parameters

Enthalpy ΔH°, free energy ΔG°, and entropy ΔS° changes were determined using Equations (12)–(14):

$$\Delta G^o = RT \ln K_D, \quad (12)$$

$$\Delta G^o = \Delta H^o - T\Delta S^o, \quad (13)$$

$$\ln K_D = \frac{-\Delta H^o}{RT} + \frac{\Delta S^o}{R}, \quad (14)$$

where K_D is the distribution coefficient and equivalent to the preliminary Pb(II) concentration (C_o) divided by the final Pb(II) concentration (C_e).

Figure 12 shows a linear plot of ln K_D versus 1/T. The thermodynamic parameters were determined and are presented in Table 4. The negative value of ΔH° indicates the exothermic nature of the adsorption process. The positive value of entropy (ΔS°) proposes an increased randomness at the solid–solution interface. Negative values of Gibbs free energy (ΔG°) prove that the adsorption process is spontaneous, which becomes more positive with an increase in temperature. Therefore, this indicates that less adsorption occurs at elevated temperatures. This is in good agreement with the results obtained from Figure 10c.

Table 4. Thermodynamic parameters of the adsorption of Pb(II) ions on AILP.

T, K	K_D	ΔG, kJ/mol	ΔS, J/mol K	ΔH, kJ/mol
298	24.70	−8.0		
308	19.99	−7.6	40	−18.6
318	15.40	−7.0		

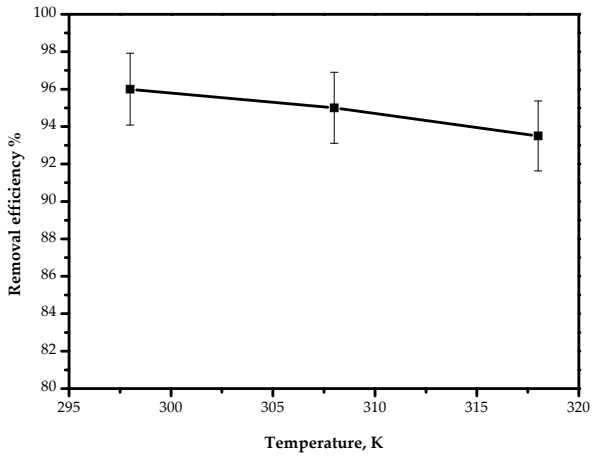

Figure 11. Effect of the temperature on the removal of Pb(II) ions by AILP.

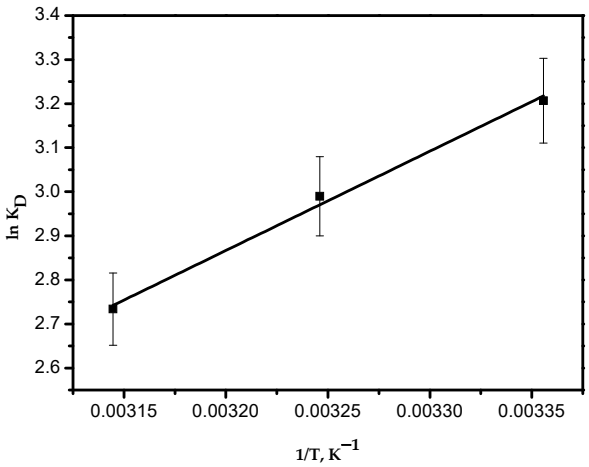

Figure 12. Plot of ln K_D versus 1/T.

3.11. Reusability of AILP

The results of reusing the AILP are presented in Figure 13. It appeared that the adsorption effectiveness of the AILP decreased gradually with the reusability. The results confirm that the AILP can be efficiently recycled 2–3 times when removing Pb(II) ions from their aqueous solutions. The adsorption efficiency of the AILP decreased to 68.5% when it was reused for a fifth time.

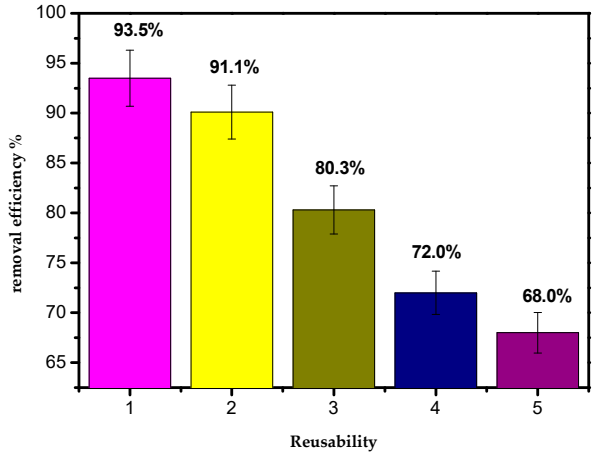

Figure 13. The reusability of AILP.

3.12. Possible Adsorption Mechanism

The adsorption of Pb(II) ions on the AILP surface possibly jointly occurs by means of chemical interactions and physisorption. The ATR-FT-IR analysis proves that a Pb-O bond is formed after the adsorption process; on the other hand, values of ΔG° and b_t suggest a physisorption process.

3.13. Comparison of AILP with Other Sorbents

An evaluation of q_{max} of the AILP according to the reported q_{max} values for other biosorbents is shown in Table 5. Variances in q_{max} can be attributed to the specific nature and properties of each adsorbent, surface area, and construction of the adsorbent. Making this comparison with other adsorbents confirms that AILP is a good and promising adsorbent.

Table 5. Comparison of AILP and other biosorbents.

Adsorbent	q_{max}	Kinetics	Isotherm	References
AILP	39.7	2nd order	Frendluich	This study
Juniperus procera	30.3	2nd order	Langmuir	[1]
Coconut shell	22.6	1st order	Langmuir	[26]
Pumpkin seed shell	14.3	2nd order	Langmuir	[27]
Cashew nut shell	17.8	2nd order	Frendluich	[28]
Polypyrrole-based AC	50.0	2nd order	Frendluich	[29]
Polygonum orientale Linn	98.4	2nd order	Langmuir	[30]

4. Conclusions

In this study, *Azadirachta indica* leaves' powder (AILP), which is a natural adsorbent material, eco-friendly, and inexpensive, was investigated. AILP was used for the removal of Pb(II) ions from aqueous solution. The removal efficiency reached above 95%. The powder of the leaves spontaneously retained considerable amounts of Pb(II) ions. The maximum adsorption capacity for neem leaves was determined as being 39.7 mg/g. Experimental investigations defined the optimum conditions for the competent removal of 50 mg/L of Pb(II) ion to be 0.60 g, 40 min of contact time, and a pH of 7. These are significant characteristics for this tested adsorbent, making it an excellent choice for cleaning polluted water due to it (1) being a natural material and (2) cost-effective, as it requires no chemical treatment; (3) its availability, with this material being abundantly available in the region; and (4) its effectiveness, with it being capable of removing Pb(II) ions with a high efficiency. These positive characteristics would make this adsorbent a suitable candidate for removing other poisonous metal ions.

Author Contributions: Conceptualization A.E. and I.H.A.; methodology, A.E.; validation, E.I.B.; formal analysis, E.I.B.; investigation A.E.; resources, A.E.; writing—original draft preparation, A.E. and I.H.A.; writing—review and editing, E.I.B. and I.S.; project administration, I.H.A.; funding acquisition, A.B.E.; supervision, B.K. All authors have read and agreed to the published version of the manuscript.

Funding: The authors extend their appreciation to the Deanship of Scientific Research at King Khalid University for funding this work through a research groups program under grant number R.G.P.1/139/40.

Institutional Review Board Statement: Not applicable.

Informed Consent Statement: Not applicable.

Data Availability Statement: Data is contained within the article.

Conflicts of Interest: The authors declare no conflict of interest.

References

1. Ali, I.H.; Al Mesfer, M.K.; Khan, M.I.; Mohd, M.; Alghamdi, M.M. Exploring Adsorption Process of Lead (II) and Chromium (VI) Ions from Aqueous Solutions on Acid Activated Carbon Prepared from *Juniperus procera* Leaves. *Processes* **2019**, *7*, 217. [CrossRef]
2. Fu, F.; Wang, Q. Removal of heavy metal ions from wastewaters: A review. *J. Environ. Manag.* **2011**, *92*, 407–418. [CrossRef]
3. Morosanu, I.; Teodosiu, C.; Paduraru, C.; Ibanescu, D.; Tofan, L. Biosorption of lead ions from aqueous effluents by rapeseed biomass. *New Biotechnol.* **2017**, *39*, 110–124. [CrossRef]
4. Gupta, V.K.; Rastogi, A. Biosorption of lead from aqueous solutions by green algae Spirogyra species: Kinetics and equilibrium studies. *J. Hazard. Mater.* **2008**, *152*, 407–414. [CrossRef]
5. Amer, M.W.; Ahmad, R.A.; Awwad, A.M. Biosorption of Cu(II), Ni(II), Zn(II) and Pb(II) ions from aqueoussolution by *Sophora japonica* pods powder. *Int. J. Ind. Chem.* **2015**, *6*, 67–75. [CrossRef]
6. Das, D.; Chakraborty, S.; Bhattacharjee, C.; Chowdhury, R. Biosorption of lead ions (Pb^{2+}) from simulated wastewater using residual biomass of microalgae. *Desalination Water Treat.* **2016**, *57*, 4576–4586. [CrossRef]
7. Papirio, S.; Frunzo, L.; Mattei, M.R.; Ferraro, A.; Race, M.; D'Acunto, B.; Esposito, G. Heavy metal removal from wastewaters by biosorption: Mechanisms and modeling. In *Sustainable Heavy Metal Remediation*, 1st ed.; Rene, E.R., Sahinkaya, E., Lewis, A., Lens, P.N.L., Eds.; Springer: Berlin/Heidelberg, Germany, 2017; Volume 8, pp. 25–63.
8. Xuan, Z. Study on the equilibrium, kinetics and isotherm of biosorption of lead ions onto pretreated chemically modified orange peel. *Biochem. Eng. J.* **2006**, *31*, 160–164. [CrossRef]
9. Mungasavalli, P.D.; Viraraghavan, T.; Jin, Y. Biosorption of chromium from aqueous solutions by pr treated Aspergillus niger: Batch and column studies. *Colloids Surf. A Physicochem. Eng. Asp.* **2007**, *301*, 214–223. [CrossRef]
10. Ucun, H.; Kemal, B.Y.; Kaya, Y.; Cakici, A.; Algur, O.F. Biosorption of lead (II) from aqueous solution by cone biomass of *Pinus sylvestris*. *Desalination* **2003**, *154*, 233–238. [CrossRef]
11. Singanan, M. Removal of lead (II) and cadmium (II) ions from wastewater using activated biocarbon. *Sci. Asia* **2011**, *37*, 115–119. [CrossRef]
12. Sulaymon, A.H.; Mohammed, A.A.; Al-Musawi, T.J. Competitive biosorption of lead, cadmium, copper, and arsenic ions using algae. *Environ. Sci. Pollut. Res.* **2013**, *20*, 3011–3023. [CrossRef] [PubMed]
13. Verma, A.; Kumar, S.; Kumar, S. Biosorption of lead ions from the aqueous solution by *Sargassum filipendula*: Equilibrium and kinetic studies. *J. Environ. Chem. Eng.* **2016**, *4*, 4587–4599. [CrossRef]
14. Barka, N.; Abdennouri, M.; El Makhfouk, M.; Qourzal, S. Biosorption characteristics of cadmium and lead onto eco-friendly dried cactus (Opuntia ficus indica) cladodes. *J. Environ. Chem. Eng.* **2013**, *1*, 144–149. [CrossRef]
15. Iram, S.; Shabbir, R.; Zafar, H.; Javaid, M. Biosorption and bioaccumulation of copper and lead by heavy metal-resistant fungal isolates. *Arab. J. Sci. Eng.* **2015**, *40*, 1867–1873. [CrossRef]
16. Okoye, A.; Ejikeme, P.; Onukwuli, O. Lead removal from wastewater using fluted pumpkin seed shell activated carbon: Adsorption modeling and kinetics. *Int. J. Environ. Sci. Technol.* **2010**, *7*, 793–800. [CrossRef]
17. Senthil, K.P. Adsorption of lead (II) ions from simulated wastewater using natural waste: A kinetic, thermodynamic and equilibrium study. *Environ. Prog. Sustain. Energy* **2014**, *33*, 55–64. [CrossRef]
18. Abadian, S.; Rahbar-Kelishami, A.; Norouzbeigi, R.; Peydayesh, M. Cu(II) adsorption onto Platanus orientalis leaf powder: Kinetic, isotherm, and thermodynamic studies. *Res. Chem. Intermed.* **2015**, *41*, 7669–7681. [CrossRef]
19. Peydayesh, M.; Isanejad, M.; Mohammadi, T.; Jafari, S.M.R.S. Assessment of Urtica as a low-cost adsorbent for methylene blue removal: Kinetic, equilibrium, and thermodynamic studies. *Chem. Pap.* **2015**, *69*, 930–937. [CrossRef]
20. Al-Hashemi, Z.S.S.; Hossain, M.A. Biological activities of different neem leaf crude extracts used locally in Ayurvedic medicine. *Pac. Sci. Rev. A Nat. Sci. Eng.* **2016**, *18*, 128–131. [CrossRef]
21. Elkhaleefa, A.; Ali, I.H.; Brima, E.I.; Elhag, A.B.; Karama, B. Efficient Removal of Ni(II) from Aqueous Solution by Date Seeds Powder Biosorbent: Adsorption Kinetics, Isotherm and Thermodynamics. *Processes* **2020**, *8*, 1001. [CrossRef]
22. El-Zahhar, A.A.; Idris, A.M. Mercury(II) decontamination using a newly synthesized poly(acrylonitrile-acrylic acid)/ammonium molybdophosphate composite exchanger. *Toxin Rev.* **2020**, *39*, 1–13. [CrossRef]
23. Khan, M.I.; Al Mesfer, M.K.; Danish, M.; Ali, I.H.; Shoukry, H.; Patel, R.; Gardy, J.; Rehan, M. Potential of Saudi natural clay as an effective adsorbent in heavy metals removal from wastewater. *Desalination Water Treat.* **2019**, *15*, 140–151. [CrossRef]
24. Eleryan, A.; El Nemr, A.; Abubakr, M.; Idris, A.M.; Alghamdi, M.M.; El-Zahhar, A.A.; Tarek, O.; Said, T.O.; Sahlabji, T. Feasible and eco-friendly removal of hexavalent chromium toxicant from aqueous solutions using chemically modified sugarcane bagasse cellulose. *Toxin Rev.* **2020**, *39*, 1–12. [CrossRef]
25. Kavitha, G.; Sridevi, V.; Venkateswarlu, P.; Babu, N.C. Biosorption of chromium from aqueous solution by *Gracilaria corticata* (Red Algae) and its statistical analysis using response surface methodology. *Open Access Libr. J.* **2016**, *3*, 1–32. [CrossRef]
26. Taha, M.F.; Kiat, C.F.; Shaharun, M.S.; Ramli, A. Removal of Ni(II), Zn(II) and Pb(II) ions from single metal aqueous solution using activated carbon prepared from rice husk. *Int. J. Environ. Ecol. Eng.* **2011**, *5*, 855–860.
27. Xiong, C.; Yao, C. Synthesis, characterization and application of triethylenetetraamine modified polystyrene resin in removal of mercury, cadmium and lead from aqueous solutions. *Chem. Eng. J.* **2009**, *155*, 844–850. [CrossRef]
28. Xiong, C.; Yao, C. Preparation and application of acrylic acid grafted polytetraflouroethylene fiber as a weak acid cation exchanger for adsorption of Er(III). *J. Hazard. Mater.* **2009**, *170*, 1125–1132. [CrossRef]

29. Abdulaziz Ali Alghamdi, A.A.; Al-Odayni, A.; Saeed, W.S.; Al-Kahtani, A.; Alharthi, F.A.; Aouak, T. Efficient Adsorption of Lead (II) from Aqueous Phase Solutions Using Polypyrrole-Based Activated Carbon. *Materials* **2019**, *12*, 1–16.
30. Wang, L.; Zhang, J.; Zhao, R.; Li, Y.; Li, C.; Zhang, C. Adsorption of Pb (II) on activated carbon prepared from Polygonum orientale Linn.: Kinetics, isotherms, pH, and ionic strength studies. *Bioresour. Technol.* **2010**, *101*, 5808–5814. [CrossRef] [PubMed]